EUROPEAN JOURNAL OF COMPUTATIONAL MECHANICS
2018, VOL. 27, NO. 4, 322–341
https://doi.org/10.1080/17797179.2018.1550962

Taylor & Francis
Taylor & Francis Group

Check for updates

Minimising drag coefficient of a hatchback car utilising fractional factorial design algorithm

Mehrdad Vahdati, Sajjad Beigmoradi and Alireza Batooei

Mechanical Engineering Faculty, K. N. Toosi University of Technology, Tehran, Iran

ABSTRACT

Aerodynamic force is known as one of the most important attributes, which has significant weight on fuel consumption and vehicle performance. In this paper, minimising drag coefficient is performed considering modification of rear end factors. To this end, five geometrical parameters of a hatchback car are chosen as design factors in two levels: (1) rear spoiler length, (2) rear spoiler angle, (3) rear diffuser angle, (4) boat tail angle (5) fifth door height. Main and interaction effects of these factors on drag coefficient are investigated using design of experiments and optimum level for each parameter is achieved. Computational fluid dynamic method is applied to evaluate air stream around the car. To reduce the number of simulations fraction, factorial design algorithm is applied which decreased the number of case studies to half. Characteristics of airflow around optimum car model are discussed and reported at the end.

ARTICLE HISTORY
Received 4 March 2018
Accepted 19 November 2018

KEYWORDS
Vehicle aerodynamics; drag reduction; fractional factorial design; computational fluid dynamics

1. Introduction

Airflow around running vehicles can be studied from different aspects such as fuel consumption, performance, stability and aerodynamic noise. For this matter, researchers are motivated to continue their studies on airflow around car or generic car from previous decades up to now.

Aljure, Lehmkuhl, Rodriguez and Oliva (2014) have evaluated ability of different turbulence models to simulate airflow around two simplified cars. They have surveyed the structure of flow in detail around the cars for different Large Eddy Simulation models. Huminic and Huminic (2017) have studied the effect of underbody diffuser for a generic hatchback car model. They have considered length and angle of diffuser as two variables in the ranges which are applicable for hatchback cars. They have observed vortices that are generated from wheelhouses play important role on the flow pattern of the underbody diffuser. Their results show that the lift of the bluff body on wheels decreases with increasing diffuser length and diffuser angle. Moreover, they have claimed that there is a possibility of

CONTACT Sajjad Beigmoradi s.beigmoradi@email.kntu.ac.ir
© 2018 Informa UK Limited, trading as Taylor & Francis Group

reaching a drag minimum over the range of diffuser angle and normalised diffuser length tested in the study.

Beigmoradi, Hajabdollahi and Ramezani (2014) have investigated optimum parameters of a simplified car model considering aerodynamic drag and noise objects. They have used numerical simulations beside genetic algorithm for this matter. They have discussed flow characteristics around optimum models. Corallo, Sheridan and Thompson (2015) have investigated the interaction between the longitudinal c-pillar vortices the airflow over the rear slant surfaces for a simplified car model with different aspect ratios. They have found out that not only aspect ratio effects on drag coefficient but increasing the aspect ratio causes separation of the flow completely and variation of c-pillar vortex strength. Hanfeng, Yu, Chao and Xuhui (2016) have investigated the influences of different deflectors on aerodynamic drag of a simplified car model. They have installed deflectors with different height and width size at side and leading edge of slant. They have observed that deflector at leading edge of slant changes the near wake of model similar to the rear end of the model with larger slant angle. Moreover, they have claimed that for smaller slant angle of model installing the deflector at leading edge is more efficient in drag reduction. Thacker, Aubrun, Leroy and Devinant (2012) have studied the effect of cancelation flow separating on aerodynamic drag. They have considered two different simplified car models: (1) with sharp edge at connection of roof and slant angle (2) rounded edge at connection of roof and slant angle. They have indicated that omitting separation on rear slant angle due to rounding the edge causes for weaker drag. Song et al. (2012) have studied aerodynamic optimisation of rear end of a sedan car. They have considered six parameters of rear part as design variables and utilised artificial neural network and computational fluid dynamics (CFD) as tools for this matter. They have concluded that by choosing optimum variables, the aerodynamic performance could be enhanced 5.64% in comparison with base line design. Khaled, El Hage, Harambat and Peerhossaini (2012) have investigated some parameters of a simplified car model on aerodynamic drag. They have performed some experiments for this matter and at the end they have reported their solutions for drag reductions. Grandemange et al. (2015) have optimised the simplified square back of car model. They have found out that top and bottom chamfer angle play significant role on aerodynamic drag. So, changing these chamfer angle, they achieved optimised shape in aspect of aerodynamic drag. Ha, Jeong and Obayashi (2011) have surveyed aerodynamic performance of a generic pickup car utilising numerical simulation and experimental test. They have added a rear flap to the roof of their model and investigated the role of the length and angle of this part on pressure and drag coefficients. They have suggested optimum downward angle and

length of the rear flap to maximise drag reduction. Salati, Cheli and Schito (2015) and Salati, Schito and Cheli (2017) have studied the effect of some add-on parts on aerodynamic drag phenomenon for a heavy truck vehicle. They have established some add-on devices on the top and side of trailer at the front and rear end to survey which part has the most impact on drag reductions. Ha, Chun, Park and Kim (2017) have studied the airflow around small passenger car in order to improve aerodynamic performance. They have concluded that adding perforated holes on wheelhouse line can enhance drag coefficient and radiator mass flow rate by relieving the high pressure in engine compartment. Beigmoradi and Ramezani (2013) have investigated the effect rear window angle on the aerodynamic and acoustic parameters for a simplified car model. They have achieved critical angle for rear window in aspect of drag and aero-acoustic noise. Buljac, Džijan, Korade, Krizmanić and Kozmar (2016) have studied aerodynamic load and flow structure for a simplified sedan car model, when a rear wing is installed on the trunk, utilising numerical simulations. They have considered four wing heights while the angle of it was constant. They have concluded that installing rear wing at about 40% of height between trunk and roof provides optimal downforce to drag ratio. Khalighi, Jindal and Iaccarino (2012) have investigated flow field around a sport utility vehicle utilising numerical simulation. They have examined immersed boundary approach for modelling computational domain and then compare their results with experimental data. They have stated that the numerical results have good agreement with experimental test. Kim, Lee, Kim, You and Lee (2017) have surveyed the effect of cab roof fairing (CRF) on drag reduction for a heavy truck vehicle. They have observed good agreement between their numerical simulations with the experiment. They have concluded that modified CRF changes flow structure around the vehicle considerably and causes drag reduction about 20%. Tunay, Yaniktepe and Sahin (2016) have studied the flow attributes downstream of a simplified car model by numerical simulation and experimental test. They have said that, according to the characteristics of airflow on the rear slanted surface and in near wake zone, there is a significant variation in very short space in both stream-wise and vertical direction of flow. Kim and Han (2016) have investigated the effect of rear spoiler with different topologies on drag and lift force for a sedan car. They have used CFD to this end. They have chosen two spoilers among others which have better cases in aspect of drag and lift forces. Beigmoradi (2015) has obtained optimum levels of the rear end parameters for a simplified car model considering aerodynamic drag and noise. Beigmoradi has applied CFD to survey airflow structure around the models beside Taguchi algorithm to find optimum level of variables.

As studying aerodynamic performance is a time and cost consuming procedure for both test and simulation, researchers are looking for solutions to decrease these expenses. Applying simplified models or using optimisation algorithms are some keys for this problem. In this work, application of fractional factorial algorithm for aerodynamic assessment of a hatchback is introduced that can reduce the number of computations significantly.

2. Background theory

2.1. Flow equations

In this study, 3D airflow around the vehicle is supposed to be incompressible. Therefore, Navier–Stokes equations with a turbulence model are employed for numerical simulation. The Navier–Stokes equations are

$$\frac{\partial u}{\partial x}+\frac{\partial v}{\partial y}+\frac{\partial w}{\partial z}=0 \tag{1}$$

$$u\frac{\partial u}{\partial x}+v\frac{\partial u}{\partial y}+w\frac{\partial u}{\partial z}=-\frac{1}{\rho}\frac{\partial p}{\partial x}+\frac{1}{\rho}\left[\frac{\partial \tau_{xy}}{\partial y}+\frac{\partial \tau_{xz}}{\partial z}\right]+B_x \tag{2}$$

$$u\frac{\partial v}{\partial x}+v\frac{\partial v}{\partial y}+w\frac{\partial v}{\partial z}=-\frac{1}{\rho}\frac{\partial p}{\partial y}+\frac{1}{\rho}\left[\frac{\partial \tau_{xy}}{\partial x}+\frac{\partial \tau_{yz}}{\partial z}\right]+B_y \tag{3}$$

$$u\frac{\partial w}{\partial x}+v\frac{\partial w}{\partial y}+w\frac{\partial w}{\partial z}=-\frac{1}{\rho}\frac{\partial p}{\partial z}+\frac{1}{\rho}\left[\frac{\partial \tau_{xz}}{\partial x}+\frac{\partial \tau_{yz}}{\partial y}\right]+B_z \tag{4}$$

where u, v, w are the velocity components in the x, y, z directions, correspondingly, ρ is density, p is pressure and τ is shear stress. The turbulence model used for flow simulations around the car model is realisable $k-\varepsilon$ model. Realisable model can fulfil mathematical margins on the normal stress, regardless of turbulent flows physics. Shih, Liou, Shabbir, Yang and Zhu (1995) appealed that it also can deliver superior performance for flows including rotation, boundary layers under strong adverse pressure gradients, separation and recirculation.

Transport equations for k and ε in the realisable $k-\varepsilon$ is estimated as Equations (5) and (6), respectively.

$$\frac{\partial}{\partial t}(\rho k)+\frac{\partial}{\partial x_i}(\rho k u_i)=\frac{\partial}{\partial x_i}\left[\left(\mu+\frac{\mu_t}{\sigma_k}\right)\frac{\partial k}{\partial x_j}\right]+C_k+C_b-\rho\varepsilon-Q_m+S_k \tag{5}$$

$$\frac{\partial}{\partial t}(\rho\varepsilon)+\frac{\partial}{\partial x_j}(\rho\varepsilon u_j)=\frac{\partial}{\partial x_j}\left[\left(\mu+\frac{\mu_t}{\sigma_\varepsilon}\right)\frac{\partial\varepsilon}{\partial x_j}\right]+\rho D_1 S_\varepsilon - -\rho D_2\frac{\varepsilon^2}{k+\sqrt{\nu\varepsilon}} + D_{1\varepsilon}\frac{\varepsilon}{k}C_b+S_\varepsilon \quad (6)$$

where

$D_1=\max\left[0.43,\frac{\eta}{\eta+5}\right]$, $\eta=S\frac{k}{\varepsilon}$, $S=\sqrt{2S_{ij}S_{ij}}$.

In these equations, C_k denotes the creation of turbulence kinetic energy due to the mean velocity gradients. C_b is the creation of turbulence kinetic energy due to buoyancy. Q_m represents the share of the fluctuating dilatation in compressible turbulence to the overall dissipation rate. S_k and S_ε are user-defined source terms and $D_{1\varepsilon}$ are constants. σ_k and σ_ε are the turbulent Prandtl numbers for k and ε, respectively. μ_t is eddy viscosity that for realisable model can be computed from Shih et al. (1995).

2.2. Design of experiment method

Design of experiment (DOE) method is a series of structured tests or simulations on design variables (factors) in order to find out the effect of each variable on output responses. The aim of this method is obtaining optimal configuration of the system and a formulated relationship between design variables and output responses to predict the behaviour of the system. There are some techniques in the field of DOE which choosing among them depends on system characteristics, time and cost restrictions and designer proficiency. One of these techniques is fractional factorial design which can estimate the effect of main design variables and their low order interactions with minimum number of runs.

In the k design variable problems, that each factor has two level, there is need for 2^k runs in order to survey the effect of main and interactions of variables. As the number of factors increases, the number of runs, that is required for a complete factorial design, rapidly outgrows time and costs of simulations or tests. If designer reasonably omits high-order interactions (Montgomery, 2012), information on the main variables and low-order interactions may be achieved by running only a fraction of the complete factorial design. These fractional factorial designs are among the most extensively applied types of designs for product and process design, process enhancement and industrial/business research. A one-half fraction of the 2^k design of the highest resolution may be constructed by writing down a full factorial design including the runs for a full 2^{k-1} factorial and then adding the kth factor by identifying its high and low levels with the plus and minus signs of the highest order interaction $ABC\ldots(K-1)$.

A half-one fraction for a problem with five design variables would be acquired by equating variable E to the ABCD interaction. This approach is depicted in Table 1.

Notice that the basic design always has the right number of runs (rows), but it is missing one column. The generator $I = ABC\ldots K$ is then solved for the missing column (K) so that $K = ABC\ldots(K-1)$ defines the product of plus and minus signs to use in each row to produce the levels for the kth factor. It should be noted that any interaction effect could be used to generate the column for the kth factor. However, using any effect other than $ABC\ldots(K-1)$ will not produce a design of the highest possible resolution. In Table 1, each word in treatment combination column expresses that parameter is at high level while other parameters at low level. For instance, abe is a response when A, B and E variables are at high level while C and D parameters are at low level. After running all simulations, statistical analysis should be performed in order to estimate the effect of each parameter and their interactions on output response. The effect of the interactions of K parameters can be written as $AB\ldots K$ and defined by Equation (7) (Montgomery, 2012):

$$AB\ldots K = \frac{2}{2^k}\left(Contrast_{AB\ldots K}\right) \tag{7}$$

where the contrast of $AB\ldots K$ is defined as

$$Contrast_{AB\ldots K} = (a \pm 1)(b \pm 1)\ldots(k \pm 1) \tag{8}$$

In order to do analysis of variance (ANOVA) of runs, calculation of some terms is essential. These parameters are sum of square of parameters, total sum of square, sum square of error and mean square which are calculated from Equations (9)–(12), respectively.

Table 1. Configuration of runs for one-half fraction design with five parameters.

Run	*A*	*B*	*C*	*D*	*E* = *ABCD*	Treatment combination response
1	−	−	−	−	+	e
2	+	−	−	−	−	a
3	−	+	−	−	−	b
4	+	+	−	−	+	abe
5	−	−	+	−	−	c
6	+	−	+	−	+	ace
7	−	+	+	−	+	bce
8	+	+	+	−	−	abc
9	−	−	−	+	−	d
10	+	−	−	+	+	ade
11	−	+	−	+	+	bde
12	+	+	−	+	−	abd
13	−	−	+	+	+	cde
14	+	−	+	+	−	acd
15	−	+	+	+	−	bcd
16	+	+	+	+	+	abcde

$$SS_{AB\ldots K} = \frac{1}{2^k}\left(Contrast_{AB\ldots K}\right)^2 \tag{9}$$

$$SS_T = \sum_{i=1}^{k} y_i^2 - \frac{\left(\sum y_i\right)^2}{DOF_{total}} \tag{10}$$

$$SS_{\text{error}} = SS_{\text{total}} - \sum SS_i \tag{11}$$

$$MS_i = \frac{SS_i}{DOF} \tag{12}$$

where y_i and DOF are output response and degree of freedom correspondingly. For p variables with two levels, DOF is one for each parameter/interaction and $2^p - 1$ for total DOF. Defining $F = \frac{MSi}{MS_{error}}$ and comparing with F_0 (Montgomery, 2012), the effect of each parameter can be achieved.

Moreover, regression equation based on the main effects and low order interaction is

$$y_i = \beta_0 + \sum_{i=1}^{p} \beta_i x_i + \sum_{i=1}^{p} \sum_{j=1}^{p} \beta_{ij} x_i x_j \tag{13}$$

In Equation (13), β_i and β_{ij} are regression coefficients which are the half of the effects (Equation 1) for each main effect or interaction. Also, x_i and y_i are design variable i and output response, respectively.

The standard analysis method for an unreplicated two-level factorial design is the normal plot of the estimated factor effects. Unreplicated designs are extensively employed practically. Many formal analysis procedures have been suggested to overcome the subjectivity of the normal probability plot. The technique proposed by Lenth (1989) has a good ability to identify significant effects (Montgomery, 2012). According to this method, for a 2^k factorial design with m contrast (c_1, c_2, … c_m) in which m equals to $2^k - 1$, variance of a contrast could be estimated from smallest (absolute value) contrast. To this end, considering $s_0 = 1.5 \times median(c_j)$, 'pseudo-standard error' (PSE) equals to $(1.5 \times \text{median}(|c_j| : |c_j| < 2.5s_0)$. According to Lenth's study, this term is a reasonable estimator of contrast when there are a few significant effects. The PSE is applied to referee the importance of contrasts. Normal plot is a line with slop1/PSE which the effects with an absolute value exceeding the margin error (ME) are known as significant factors. Each contrast could be compared with ME which is $\text{ME} = t_{\lambda,d} \times \text{PSE}$, where $d = m/3$ and the percentage point of the t distribution is $\lambda = 1 - (1 + 0.95^{1/m})/2$ (Montgomery, 2012).

3. Modelling and simulation

3.1. Case study

In this research, enhancement of aerodynamic performance for a facelifted C-segment hatchback car is surveyed. Face lift is performed on rear end of the car to convert sedan to hatchback. Freezing other panels and parts except rear end is determined as one of the study's hard point. To this end, five design variables of rear end are chosen to be optimised. These parameters are (1) rear spoiler length (L), (2) rear spoiler angle (α), (3) fifth door height (H), (4) rear lamp boat tail angle (β) and (5) rear diffuser angle (θ). The range for variations of these parameters is determined by industrial design department. Figure 1 and Table 2 depict design variables and their variation's range, respectively.

3.2. Mesh generation

Simulation of airflow pattern around the car in virtual wind tunnel is conducted applying CFD method. For this matter, a domain with 25091mm × 4288mm × 4288mm is determined as virtual wind tunnel

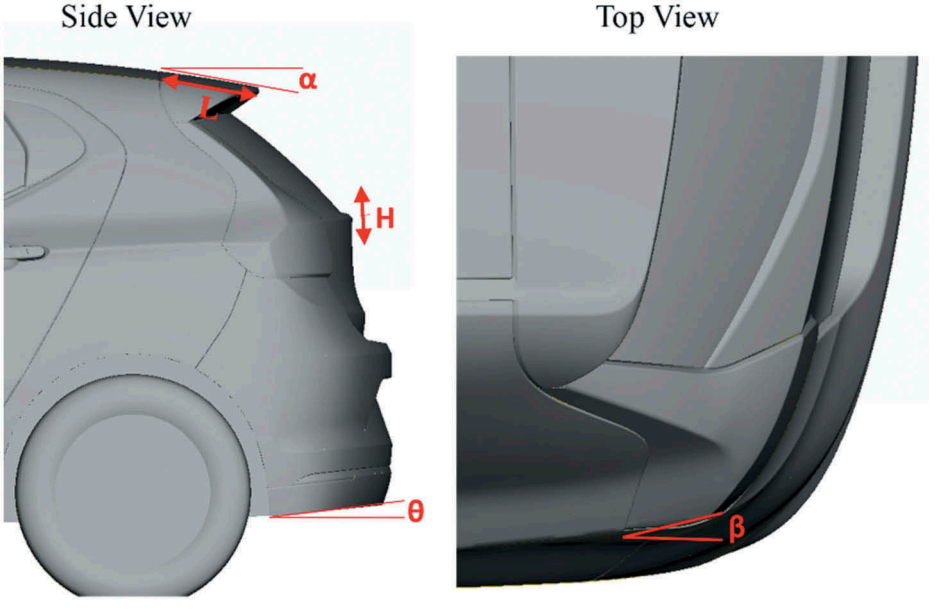

Figure 1. Configuration of rear end and its design variables.

Table 2. Range of variations for design variables.

	Spoiler angle (α)	Spoiler length (L)	5th door height (H)	Boat tail angle (β)	Diffuser angle (θ)
Low level	−20	220	−50	0	0
High level	20	290	50	20	30

and the car model is positioned in 5270mm from the flow inlet. First-order tria CFD and Hexa interior mesh are employed to generate surface and volumetric networks, respectively. Size boxes around the car and the rear end are created to control the size of elements in near the car model. Finer mesh around and at the rear end of the car model is required to increase accuracy of flow calculation around the model and detecting wakes at this region. Figure 2 shows the position of the car model in computational domain and meshing around it.

To provide accurate CFD model, different aspects of mesh generation techniques should be considered, some of the main points are as follows:

- Independency of grids in aspect of size and number.
- Choosing appropriate boundary layers around the car that can detect the velocity near the walls precisely and meet the $y+$ target range according to turbulence model. As in this work, K-Epsilon realisable turbulence model is chosen, the appropriate range is about $20 < y+ < 200$ (Connor, Kharazi, Walter, & Martindale, 2006).

So, the size and number of meshes are chosen by considering these limitations. Figure 3 and Table 3 depict the drag coefficient withstand number of grids to choose suitable mesh size and number.

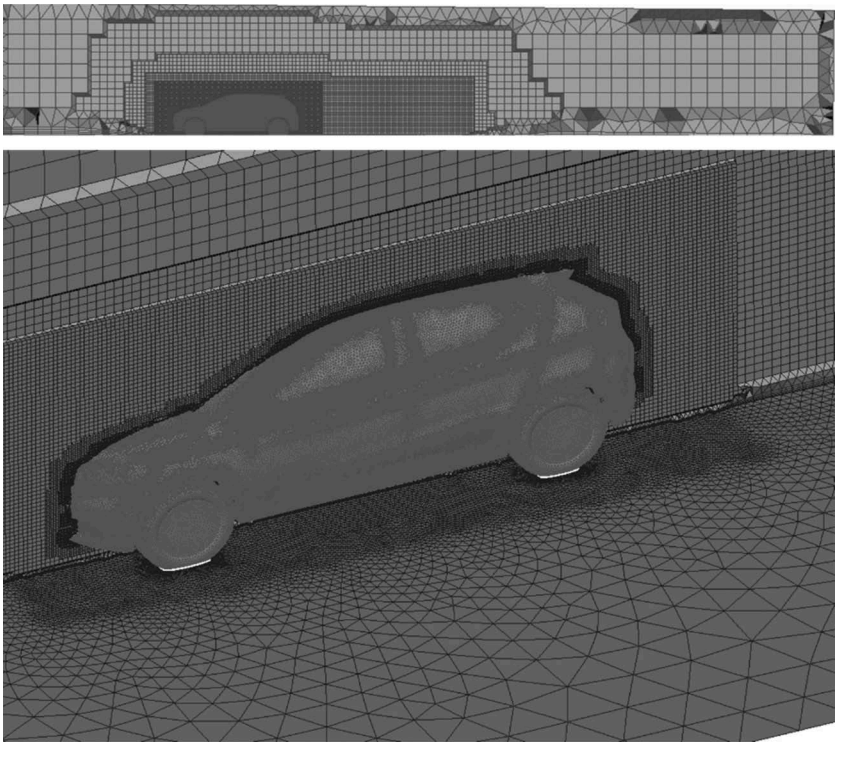

Figure 2. Position of car model in wind tunnel and meshing around the model.

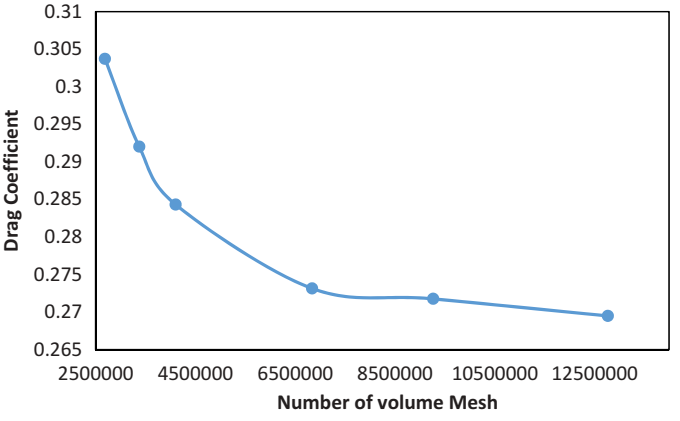

Figure 3. Drag coefficient versus number of grids.

Table 3. Drag coefficient versus number of grids for different cases.

Case number	Grid number	Cd
Case 1	2685914	0.30371
Case 2	3374018	0.29201
Case 3	4103259	0.284312
Case 4	6839319	0.2731434
Case 5	9270403	0.2717526
Case 6	12773925	0.269482

Comparison of different cases shows that there is no significant change between cases 4, 5 and 6. The variation between case 4 and 6 in drag coefficient is about 1.3%. So, considering time and cost of simulations, the grid size of case 4 is chosen in this work. Moreover, by choosing appropriate boundary layers, $y+$ parameter meets the specified target range for the main car model (Figure 4).

Morphing technique is utilised with the aim of changing the geometric parameters of the rear end. This method can be used to modify the geometry of the model without significant variation in mesh quantity. To this end, different numbers of morph boxes are created around each parameter to cover requirements for the modifications. Total number of morph boxes is 60.

3.3. Boundary condition

As the body is symmetry, half of car and tunnel are modelled for the flow simulations to reduce time and cost of consumption. $38.89\frac{m}{s}$ is set for input flow which is top speed of the vehicle considering 0.025% of turbulent intensity and viscosity ratio. Stationary wall with no motion is considered for the body and rotational moving walls are set for tires. Moreover, moving wall and no motion with zero shear stress are defined for road and tunnel

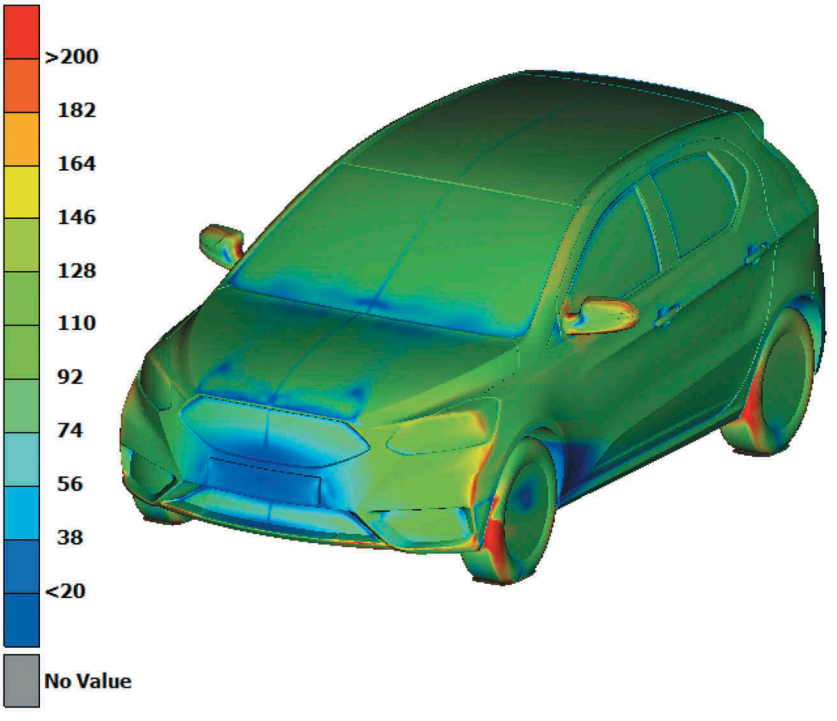

Figure 4. $y+$ contour around the model.

side walls correspondingly. Density and viscosity of the air are $1.19\frac{kg}{m^3}$ and $1.79 \times 10^{-5}\frac{kg}{m.s}$, respectively. The $k-\varepsilon$ realisable turbulence model is hired for simulations considering standard wall function, which has an appropriate ability in estimating flow separation and formation of vortices.

4. Result and discussion

4.1. Validation of turbulence model

Ahmed bluff body (Ahmed & Ramm, 1984) (Figure 5) is a generic car model that provides a good perspective for investigating aerodynamic behaviour of hatchbacks. Variations of rear slant angle (α) deliver different drag coefficients that express importance of rear end of hatchbacks on aerodynamic performance. To find out accuracy of the turbulence model, numerical simulations are conducted for Ahmed model in primary phase and numerical results are compared with experiments.

It is observed that the computed drag coefficient using $k-\varepsilon$ realisable turbulence model with standard wall function is in good agreement with the experimental results reported in Strachan, Knowles and Lawson (2007). The numerically obtained drag coefficients are compared with experimental results (Strachan et al., 2007) for various backlight angles and depicted in Figure 6. The

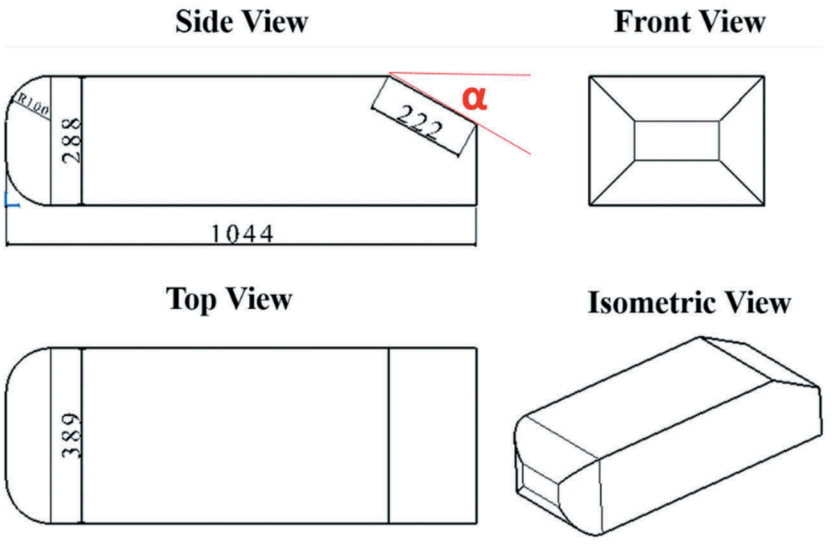

Figure 5. Ahmed bluff body in different view (dimension in mm).

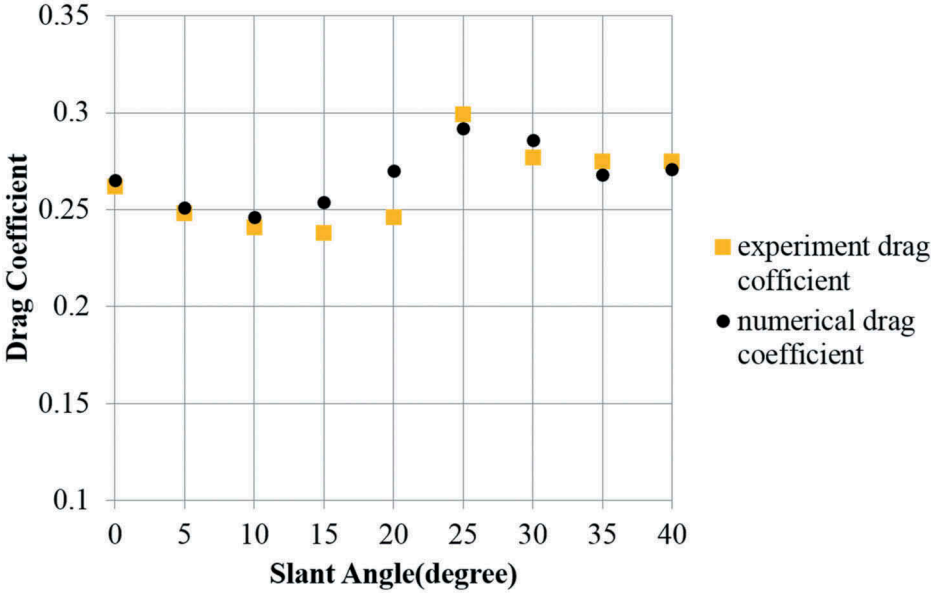

Figure 6. Comparison of numerically and experimentally obtained drag coefficients for different slant angles.

results indicate that the average deviation between the simulation and experimental results is 3.4%, which is acceptable in aspect of engineering view.

4.2. Fractional factorial results

In order to achieve minimum drag coefficient, five design variables are chosen for optimisation. Fractional factorial design based on DOE is applied to reduce time and cost of simulations. The best layout in this method is when the effect of main variables and their two order interactions can be evaluated while they are not aliased with each other. Therefore, half-fraction with resolution V prepares this condition for a problem with five design variables (Montgomery, 2012). Table 4 shows the configuration of the 16 runs for coded variables. In coded variables, each parameter in high and low level is depicted with 1 and −1, respectively. As it is mentioned in Section 3.1, level (1) for spoiler angle, spoiler length, fifth door height, boat tail angle and diffuser angle is 20°, 290 mm, 50 mm, 20° and 30°, respectively. Also, level (−1) is −20°, 220 mm, −50 mm, 0° and 0° for spoiler angle, spoiler length, fifth door height, boat tail angle and diffuser angle accordingly. Writing design variable in codded format makes interpretation of results easier than original unites (Montgomery, 2012). Sixteen runs are conducted to achieve corresponding drag coefficients and results are shown in last column of Table 4. In the next step, ANOVA for the results is performed to achieve the influence of each parameter on drag coefficient.

Normal plot of the effects from ANOVA is depicted in Figure 7. This plot provides a good estimation for the impact of design variables in unreplicated problems (Lenth, 1989). In this scheme, the effective parameters don't fall near the line. According to Figure 7, spoiler angle, spoiler length, diffuser angle, interactions between spoiler angle–diffuser angle and also spoiler angle–spoiler length have significant effect on drag coefficient. On the other hand, According to the analysis results, boat tailing of rear lamp and variation of fifth door height don't have considerable impact on drag coefficient.

Table 4. Design configurations and drag result.

Run	Spoiler angle	Spoiler length	5th Door height	Boat tail angle	Diffuser angle	Drag coefficient
1	−1	−1	−1	−1	1	0.282
2	1	−1	−1	−1	−1	0.350
3	−1	1	−1	−1	−1	0.296
4	1	1	−1	−1	1	0.417
5	−1	−1	1	−1	−1	0.303
6	1	−1	1	−1	1	0.392
7	−1	1	1	−1	1	0.277
8	1	1	1	−1	−1	0.372
9	−1	−1	−1	1	−1	0.300
10	1	−1	−1	1	1	0.390
11	−1	1	−1	1	1	0.287
12	1	1	−1	1	−1	0.370
13	−1	−1	1	1	1	0.285
14	1	−1	1	1	−1	0.356
15	−1	1	1	1	−1	0.295
16	1	1	1	1	1	0.411

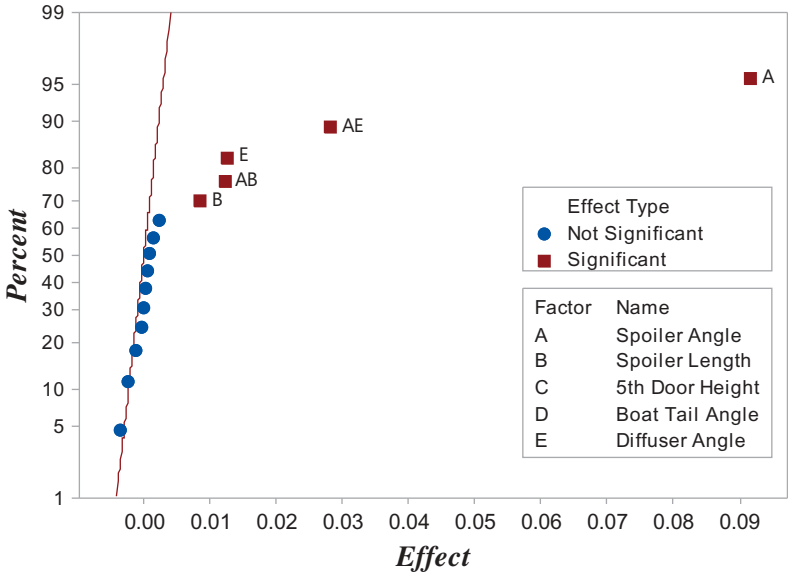

Figure 7. Normal plot of the effects ($\alpha = 0.05$).

One the most advantages of fractional factorial design is investigating the effect of main parameters and their interactions simultaneously. According to ANOVA, spoiler angle is one of the parameters that has significant impact on aerodynamic drag. According to Figures 8 and 9, setting spoiler angle in low level provides minimum drag force. For spoiler length parameter, even though Figure 8 shows choosing this parameter in low level delivers low drag, spoiler angle and length interaction in Figure 9 discard this point. According to Figure 9 considering spoiler length in high level reduces drag coefficient. In this situation, interaction effect has superiority to main effect plot. According to Figure 9, for diffuser angle similar to spoiler length, variation of drag in diffuser–spoiler angle interaction plot is significant and setting diffuser angle in high level causes for smaller drag coefficient. Comparing Figures 8 and 9, there is a conflict for plot trend in main and interaction figures but priority of interaction effect to main effect caused for choosing diffuser angle at top level. Regarding Figure 8, fifth door and boat tail angle don't have considerable influence on drag coefficient but in view of their interactions with spoiler angle (Figure 9), choosing fifth door height and boat tail angle at top and low level respectively generates lower drag coefficient.

After identification of important parameters, modifying model is performed to obtain regression model according to crucial terms. To this end, unimportant terms are omitted from ANOVA and the analysis is repeated to find regression model with key terms. Regression model that is obtained from modified ANOVA is written as

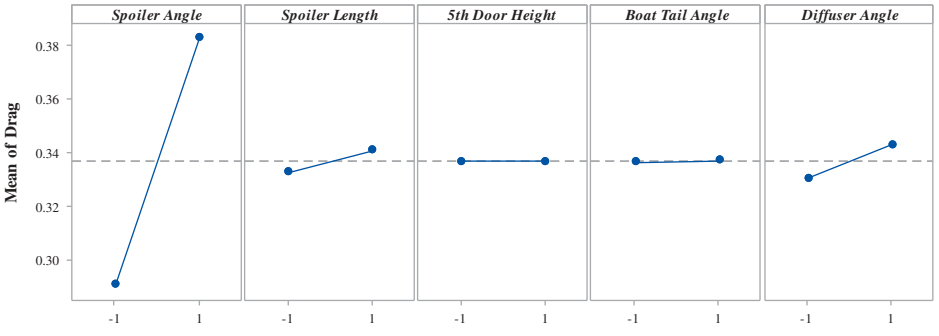

Figure 8. Main effects plot for drag.

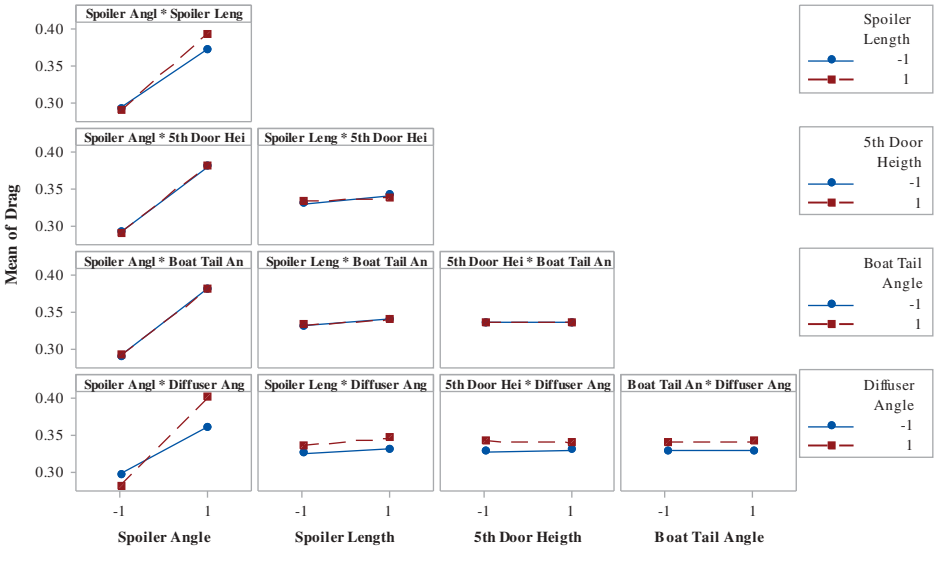

Figure 9. Interaction plot for drag (fitted means).

$$C_D = 0.336538 + (0.045795 \times \alpha) + (0.004129 \times L) + (0.006208 \times \theta) + (0.006017 \times \alpha \times L) + (0.014054 \times \alpha \times \theta) \quad (14)$$

Equation (14) includes the crucial terms of main effect and their interactions. As it is seen in this equation, coefficient of spoiler angle has maximum value in comparison with other coefficients. In can be interpreted that variation of spoiler angle has the most important role on drag coefficient and interaction of spoiler and diffuser angle ranks second. It shows that to have minimum drag, spoiler angle should take its lowest value.

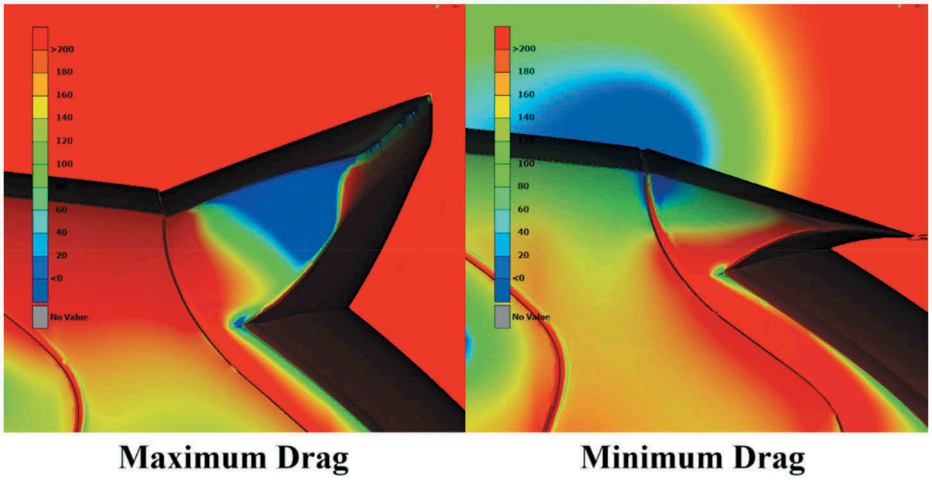

Figure 10. Pressure (pascal) around the model.

4.3. Aerodynamic performance of optimal model

In this section, characteristics of airflow around the optimal model, which is achieved from fractional factorial method, are compared with the run with maximum drag coefficient. According to the numerical simulations pressure, drag has the most contribution to total drag. For optimal model pressure and viscous, drags are 0.254 and 0.024, respectively, which indicates about 90% of total drag is pressure drag. Regarding to Figure 10, significant pressure variation exists at the junction of roof and spoiler. For optimal model, pressure decreases considerably in comparison with roof upstream pressure, which can play significant role in drag reduction. But for a model with maximum drag, the pressure in this region significantly is bigger than optimal model.

Pressure magnitude alongside rear spoiler for optimal and maximal drag is depicted in Figure 11. For the model with minimum drag, the air pressure at vicinity of spoiler junction with roof is negative and it guides flow alongside the spoiler. Moving towards the tip of the spoiler in this case, pressure grows up due to positive back pressure at the rear end. For the model with maximum drag, an opposite trend for pressure values on the spoiler is observed. The air pressure at the spoiler junction to the roof has maximum value due to decrease velocity of flow at this zone. For the maximum drag model, moving towards the tip of the spoiler decreases the pressure values. It is detected that pressure values at upper face of spoiler for optimum model are less than the model with maximum drag. Pressure difference decreases by moving towards the tip of spoiler.

According to numerical simulations, tuning spoiler angle has significant effect on flow separation and vortex size. The importance of spoiler parameter

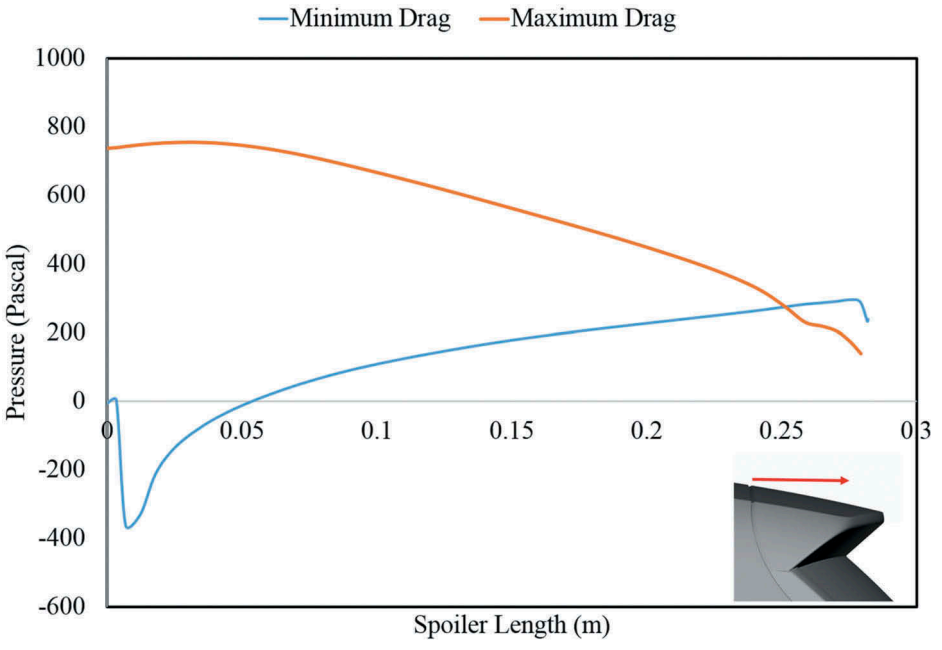

Figure 11. Pressure distribution along spoiler.

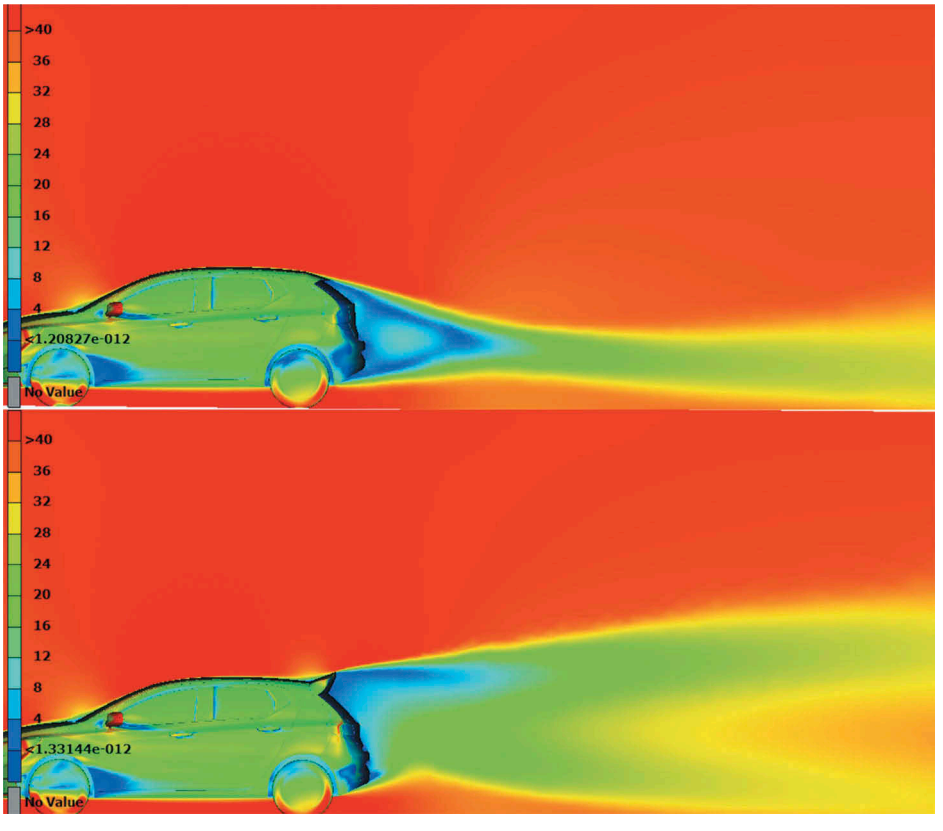

Figure 12. Velocity (m/s) contour for the car with minimum drag (up) and maximum drag (bottom).

on drag coefficient which is mentioned in the previous section can be seen in the Figure 12. According to Figure 12, for optimal shape, separation of flow occurs at the tip of spoiler and the size of generated wake at the rear end of the model is significantly smaller in comparison with other models. As it is shown in this figure, for a model with maximum drag, the size of vortices impacts on a large region of the rear end. In the other word, it can be concluded that spoiler angle has dominant effect on drag coefficient by minimising air pressure and streamlining the flow at rear end of the car.

Not only the spoiler angle has significant effect on wake's size, but it also can change the shape of vortices. As it is depicted in Figure 13, for optimal car model, two y-axis vortexes are generated in upper and bottom region of the rear end. The size of bottom vortex is bigger in comparison with the upper one. It shows that the effect of lower vortex in aerodynamic drag is more than upper vortex. But for a model with maximum drag, the shape and direction of vortices different from optimal model. In this case, two big x-axis vortices are generated at the rear end that circulates against each other. The size of each vortex is about the height of the model and it can produce significant drag.

5. Conclusion

In this paper, optimal shape for rear end of a hatchback model is achieved considering aerodynamic drag object. To this end, fractional factorial design based on DOE is chosen that is a time and cost-effective algorithm.

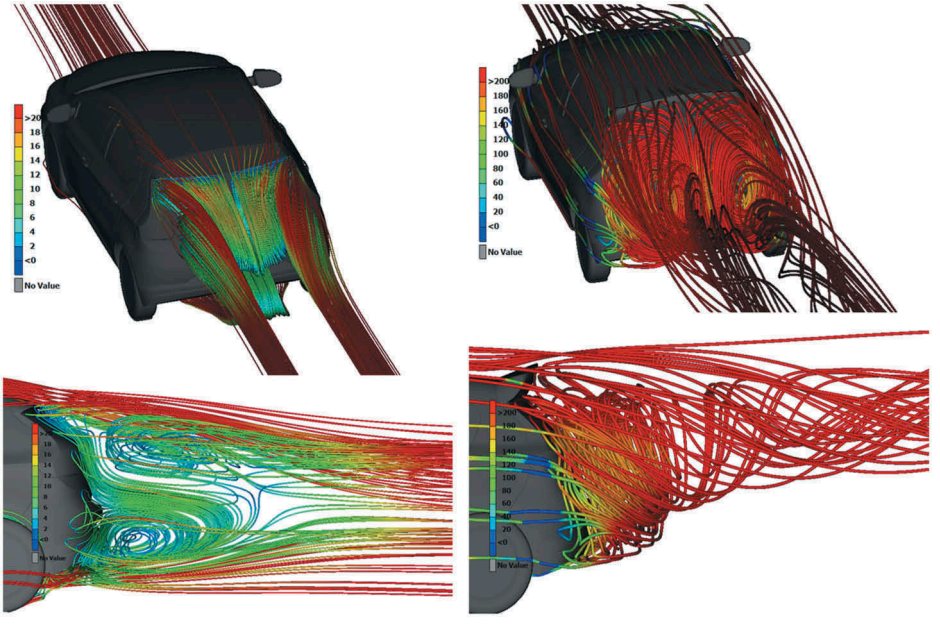

Figure 13. Streamlines based on velocity (m/s) around the car with minimum (left) and maximum (right) drag.

Contribution of five design parameters and their interaction on aerodynamic is studied. For this matter, numerical simulations are performed for suggested configurations of rear end based on optimisation algorithm and their results are reported. It is observed that surveying interactions of parameters is crucial to make accurate decision about optimum parameters. Then the regression model is derived from the results of ANOVA. It is concluded that spoiler angle has the most crucial role in the regression drag model. Interaction between spoiler and diffuser angle ranked second in this equation. Simulations show how spoiler angle effects on aerodynamic performance by changing pressure at the rear end zone. Moreover, it is perceived that not only spoiler angle has considerable influence on vortex size but it also plays an important role in the shape of vortices.

Acknowledgments

The authors would like to express their gratitude to Automotive Industries Research & Innovation Center (AIRIC) of SAIPA, for valuable support.

Disclosure statement

No potential conflict of interest was reported by the authors.

ORCID

Sajjad Beigmoradi http://orcid.org/0000-0001-8557-6508

References

Ahmed, S. R., & Ramm, G. (1984). Salient features of the time-averaged ground vehicle wake. *SAE Technical Paper*, p. 840300.

Aljure, D. E., Lehmkuhl, O., Rodriguez, I., & Oliva, A. (2014). Flow and turbulent structures around simplified car models. *Computers & Fluids*, *96*, 122–135.

Beigmoradi, S. (2015). Aerodynamic drag and noise minimization of rear end parameters in a simplified car model utilizing Robust parameter design method. *SAE Technical Paper 2015-01-1360*. doi:10.4271/2015-01-1360.

Beigmoradi, S., Hajabdollahi, H., & Ramezani, A. (2014). Multi-objective aero acoustic optimization of rear end in a simplified car model by using hybrid Robust parameter design, artificial neural networks and genetic algorithm methods. *Computers & Fluids*, *90*, 123–132.

Beigmoradi, S., & Ramezani, A. (2013). Effect of the backlight angle on the aero-acoustics of the C-Pillar. *International Review on Modelling and Simulations (IREMOS)*, *6*(3), 988–993.

Buljac, A., Džijan, I., Korade, I., Krizmanić, S., & Kozmar, H. (2016). Automobile aerodynamics influenced by airfoil-shaped rear wing. *International Journal of Automotive Technology*, *17*, 377–385.

Connor, C., Kharazi, A., Walter, J., & Martindale, B. (2006). Comparison of wind tunnel configurations for testing closed-wheel race cars: A CFD study. *SAE 2006-01-3620*.

Corallo, M., Sheridan, J., & Thompson, M. C. (2015). Effect of aspect ratio on the near-wake flow structure of an Ahmed body. *Journal of Wind Engineering and Industrial Aerodynamics*, *147*, 95–103.

Grandemange, M., Cadot, O., Courbois, A., Herbert, V., Ricot, D., Ruiz, T., & Vigneron, R. (2015). A study of wake effects on the drag of Ahmed's squareback model at the industrial scale. *Journal of Wind Engineering and Industrial Aerodynamics*, *145*, 282–291.

Ha, J., Jeong, S., & Obayashi, S. (2011). Drag reduction of a pickup truck by a rear downward flap. *International Journal of Automotive Technology*, *12*, 369–374.

Ha, S. J., Chun, U., Park, J. Y., & Kim, M. S. (2017). Enhancement of aerodynamic performance through high pressure relief in the engine room for passenger car using cfd technique. *International Journal of Automotive Technology*, *18*, 779–784.

Hanfeng, W., Yu, Z., Chao, Z., & Xuhui, H. (2016). Aerodynamic drag reduction of an Ahmed body based on deflectors. *Journal of Wind Engineering and Industrial Aerodynamics*, *148*, 34–44.

Huminic, A., & Huminic, G. (2017). Aerodynamic study of a generic car model with wheels and underbody diffuser. *International Journal of Automotive Technology*, *18*, 397–404.

Khaled, M., El Hage, H., Harambat, F., & Peerhossaini, H. (2012). Some innovative concepts for car drag reduction: A parametric analysis of aerodynamic forces on a simplified body. *Journal of Wind Engineering and Industrial Aerodynamics*, *107*, 36–47.

Khalighi, B., Jindal, S., & Iaccarino, G. (2012). Aerodynamic flow around a sport utility vehicle—Computational and experimental investigation. *Journal of Wind Engineering and Industrial Aerodynamics*, *107*, 140–148.

Kim, J. J., Lee, S., Kim, M., You, D., & Lee, S. J. (2017). Salient drag reduction of a heavy vehicle using modified cab-roof fairings. *Journal of Wind Engineering and Industrial Aerodynamics*, *164*, 138–151.

Kim, S. C., & Han, S. Y. (2016). Effect of steady airflow field on drag and downforce. *International Journal of Automotive Technology*, *17*, 205–211.

Lenth, R. (1989). Quick and easy analysis of unreplicated factorials. *Technometrics: A Journal of Statistics for the Physical, Chemical, and Engineering Sciences*, *31*, 469–473.

Montgomery, D. (2012). *Design and analysis of experiments* (8th ed.). Courier Westford from John Wiley & Sons Inc.

Salati, L., Cheli, F., & Schito, P. 2015. Heavy truck drag reduction obtained from devices installed on the trailer. *SAE International Journal of Commercial Vehicles*, *8*, 747–760. 2015-01-2898.

Salati, L., Schito, P., & Cheli, F. (2017). Wind tunnel experiment on a heavy truck equipped with front-rear trailer device. *Journal of Wind Engineering and Industrial Aerodynamics*, *171*, 101–109.

Shih, T. H., Liou, W. W., Shabbir, A., Yang, Z., & Zhu, J. (1995). A new Eddy-viscosity model for high Reynolds number turbulent flows – Model development and validation. *Computers & Fluids*, *24*(3), 227–238.

Song, K. S., Kang, S. O., Jun, S. O., Park, H. I., Kee, J. D., Kim, K. H., & Lee, D. H. (2012). Aerodynamic design optimization of rear body shapes of a sedan for drag reduction. *International Journal of Automotive Technology*, *13*, 905–914.

Strachan, R., Knowles, K., & Lawson, N. (2007). The vortex structure behind an Ahmed reference model in the presence of a moving ground plane. *Experiments in Fluids*, *42*(5), 659–669.

Thacker, A., Aubrun, S., Leroy, A., & Devinant, P. (2012). Effects of suppressing the 3D separation on the rear slant on the flow structures around an Ahmed body. *Journal of Wind Engineering and Industrial Aerodynamics*, *107*, 237–243.

Tunay, T., Yaniktepe, B., & Sahin, B. (2016). Computational and experimental investigations of the vortical flow structures in the near wake region downstream of the Ahmed vehicle model. *Journal of Wind Engineering and Industrial Aerodynamics*, *159*, 48–64.